Solar Energy Materials & Solar Cells 95 (2011) 3041–3046

Contents lists available at ScienceDirect

Solar Energy Materials & Solar Cells

journal homepage: www.elsevier.com/locate/solmat

Patternable brush painting process for fabrication of flexible polymer solar cells

Soo-Won Heo, Jang-Yong Lee, Ho-Jun Song, Ja-Ram Ku, Doo-Kyung Moon *

Department of Materials Chemistry and Engineering, Konkuk University, 1 Hwayang-dong, Gwangjin-gu, Seoul 143-701, Republic of Korea

ARTICLE INFO

Article history:
Received 24 March 2011
Received in revised form
13 June 2011
Accepted 19 June 2011
Available online 20 July 2011

Keywords:
Flexible polymer solar cells (FPSCs)
Repositionable adhesive
Patternable brush painting

ABSTRACT

The brushing painting method is one of the typical solution processes, which makes it possible to fabricate electronic devices by simply using polymers. For the fabrication of modules and large-area devices, however, a patterning process is required for each layer. Due to the problems associated with the conventional patterning, many studies have been conducted to develop new patterning . In this study, we successfully fabricated bulk heterojunction (BHJ) structured polymer solar cells (PSCs) on a plastic substrate with an active layer through the brushing painting process. In particular, flexible PSCs with hole transporting and photo-active layers formed by the repositionable adhesive-based patterning method were fabricated to produce large-area solar cells. The fabricated PSCs exhibited Jsc, Voc, FF and power conversion efficiency (PCE) values of 8.5 mA/cm^2, 0.636 V, 48.8% and 2.6%, respectively. In other words, they were more efficient than those fabricated by the spin coating method. In particular, an increase in the Jsc and FF values was observed when the series resistance (Rs) decreased to 29 Ω cm^2 while the shunt resistance (Rsh) increased to 2018 Ω cm^2.

1. Introduction

The fabrication of devices such as polymer solar cells (PSCs) [1–7], polymer light-emitting diodes (PLEDs) and organic thin-film transistors (OTFTs) as next-generation devices has attracted a great deal of attention. In fact, there have been numerous studies on this topic. The π-conjugated polymers, which are used in the active layer of these devices have good stability, good mechanical properties and excellent electro-optical properties. As they enable the solution process to be used, it is possible to fabricate low-cost and large-area devices by a simple method such as spin coating instead of vacuum deposition. For the fabrication of modules and large-area devices, however, a patterning process is required for each layer. Various patterning methods can be used, including plasma etching, plasma patterning [8,9] and laser ablation [10]. To apply the plasma patterning method, however, etching should be carried out by a plasma after forming a photoresist layer (e.g.: water soluble resist, protective parylene, etc.) as an etch mask. In addition, the application of a flexible substrate can cause the dimensional distortion of the substrate and degradation of the inherent properties [8]. Hence, various methods, which enable the polymer solution to be directly patterned have been investigated, such as ink-jet printing, slot-die coating and the roll-to-roll process [11–16].

Recently, low cost and flexible solar cells have become a reality in PSCs thanks to the increase in efficiency that was obtained following studies on their material and device structure. In particular, numerous studies have been performed on the optimization of the polymer: PCBM blend conditions, thermal treatment and related coating processes. In the studies by Li et al. [17] and Yang et al. [18], the PCE reached 4% due to the improvement in the crystallinity of P3HT after the pre/post-thermal treatment of the device that was fabricated using the spin-coating method by blending poly(3-hexylthiophene) (P3HT) and [6,6]-phenyl-C_{61}butyric acid methyl ester (PCBM). Aernouts et al. [19] fabricated PSCs, which had a pinhole free film, with PCE of 1.4% through the optimization of the polymer: PCBM blend concentration by using the ink-jet printing method. Huang et al. [20] fabricated PSCs to which the stamping method was applied with a PDMS stamp and reported a PCE of 3.2%. Wang et al. [21] reported inverted PSCs with a PCE of 3.19% by applying the stamping method that used a UV curable resin coated polycarbonate film. However, it was difficult to use them in the roll-to-roll process, because of the additional need for a complicated patterning process.

In addition, Kim et al. [22] reported an improvement in the efficiency of polymer solar cells as a result of the improved organization of P3HT afforded by a simple brush painting method. This highly ordered active layer, which was spun off from the P3HT and PCBM interfaces, exhibited improved charge transport. As a result, the PCE was increased up to 5.4% through the increase in fill factor. Also, the brush painting method makes it possible to fabricate annealing free PSCs efficiently for the mass production

* Corresponding author. Tel.: +82 2 450 3498; fax: +82 2 444 0765.
E-mail address: dkmoon@konkuk.ac.kr (D.-K. Moon).

0927-0248/$ - see front matter © 2011 Elsevier B.V. All rights reserved.
doi:10.1016/j.solmat.2011.06.029

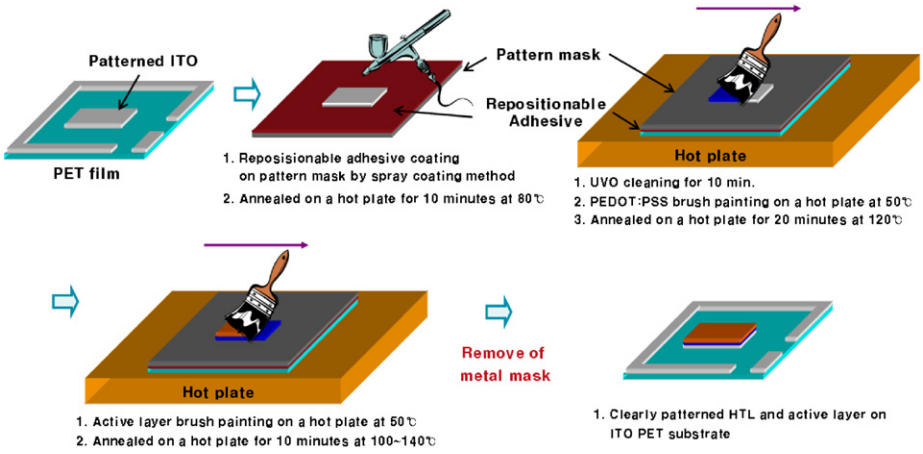

Scheme 1. Manufacturing process of flexible PSCs by patternable brush painting method.

of organic devices based on high-speed roll to roll systems [23]. In previous research, however, the brush painting method was used to fabricate a simple unit solar cell. Furthermore, there have been no studies in which sub-modules or large area cells were fabricated by applying the bush painting method to a plastic substrate. In order to make large area devices or modules, a patterning process is necessary. However, in the case where a patterned mask was used, as in the screen printing method, capillary phenomena were generated between the mask and substrate because of the low viscosity of the polymer ink. Therefore, a clean pattern could not be obtained by the conventional brush painting method. As shown in Scheme 1, a simple process, which makes it possible to pattern hole transporting and photo active layers using a repositionable adhesive was developed. Furthermore the traditional shortcomings of plastic substrates, viz. the dimensional distortion of the substrate and degradation of its inherent properties [8] were not found in this process. Moreover, this new method makes it possible to obtain very clear pattern images and to fabricate large-area PSCs. In addition, in this paper, we compared the properties of the devices fabricated using the spin-coating method, including their J–V and IPCE characteristics, and observed their surface morphology by AFM.

2. Experimental

2.1. Materials

The ITO PET film, which is used as the transparent electrode is an SKC product (PET: 125 μm, ITO:170 nm, 100 Ω/sq). As the repositionable adhesive, used in the patterning hole transporting and photo-active layers, a 3M (Model: #75 repositionable adhesive) product was used. In addition PEDOT: PSS (AI 4083) was purchased from Clevios and poly(3-hexylthiophene, P3HT), which was used as a donor material in the photo-active layer was purchased from Rieke metal. $PC_{61}BM$, an acceptor material was purchased from Nano C.

2.2. Measurements

All of the thin films were fabricated using a GMC2 spin coater (Gensys, Korea), and their thickness was measured using an alpha step 500 surface profiler (KLA-Tencor). In addition, the electro-optical properties of the fabricated device were characterized with a Keithley 2400 source meter unit (Keithley) and solar simulator (Newport). The thin film morphology of the fabricated device was measured by atomic force microscopy (PSIA XE-150).

2.3. Cleaning of PET film

To clean the PET film, sonication was performed using a detergent (Alconox® in deionized water, 10%), acetone, IPA (isopropyl alcohol) and deionized water in the order listed, for 20 min each. The moisture was removed by blowing thoroughly with N_2 gas. In order to ensure the complete removal of all of the remaining water, the ITO was baked on a hot plate for 10 min at 100 °C. For the hydrophilic treatment of the PET surface, it was cleaned for 10 min in a UVO cleaner.

2.4. Preparation of pattern mask

As shown in Fig. 2a, a square-patterned (15 mm × 15 mm) mask made of SUS 304 was prepared. After cleaning the pattern mask in the same manner as that of ITO PET, the 3M repositionable adhesive was evenly sprayed on it using the spray-coating method. After the coating process, the residual solvent was removed from the repositionable adhesive. Additionally, to increase the strength of the adhesion to the pattern mask, it was annealed at 80 °C on a hot plate for 10 min.

2.5. Fabrication of flexible PSCs by patternable brush painting method

After attaching the repositionable adhesive-coated pattern mask onto the patterned ITO PET, UVO cleaning was performed for 10 min to make the ITO PET surface hydrophilic. To form the hole transporting layer, the masked ITO PET substrate was placed on a hot plate preheated at 50 °C and PEDOT: PSS was brush painted at a speed of 1 cm/s. As a result, a film with a thickness of about 40 nm was obtained. To eliminate the residual solvent, it was annealed on a hot plate at 120 °C for about 20 min. It was possible to regulate the thickness of the PEDOT: PSS and photo-active layers by adjusting the brushing speed. Fig. 1 shows the structure of the flexible PSCs and the chemical structure of the material used in the photo-active layer. As shown in this figure, the photo active ink was blended in ortho-dichlorobenzene (ODCB) at a ratio of 1:0.6 between the donor material, P3HT, and the acceptor material, $PC_{61}BM$, at a concentration of 3.0 wt% and annealed at 90 °C for about 30 min.

After placing the PEDOT: PSS-coated ITO PET substrate onto the hot plate preheated at 50 °C, the photo-active ink was brush painted at 1 cm/s. As a result, a film with a thickness of about 130 nm was obtained. To remove the residual solvent and determine the optimum annealing temperature, it was annealed at temperatures ranging from 100 to 140 °C for about 10 min.

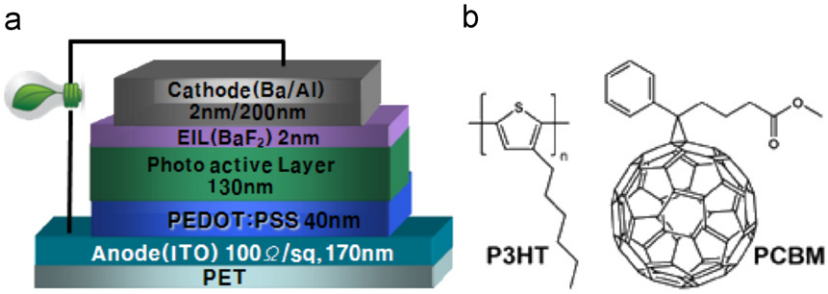

Fig. 1. Device structure of (a) flexible PSCs and (b) chemical structures of P3HT and PCBM.

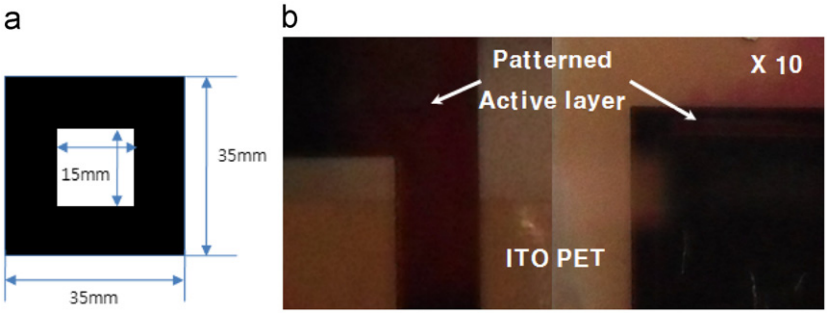

Fig. 2. Image of (a) metal mask and (b) optical microscope images of fabricated flexible PSCs by patternable brush painting method.

Then, the photo-active layer was patterned. The fabrication method is illustrated in Scheme 1 below.

2.6. Deposition of cathode

To form a cathode on the photo-active layer, BaF_2 (0.1 Å/s, 2 nm), Ba (0.2 Å/s, 2 nm) and Al (5 Å/s, 200 nm) were thermally deposited in a high vacuum chamber (1×10^{-6} torr or less) in that order. To protect the organic material layers and electrode from H_2O and O_2, a getter was attached to the inside of the glass cover. Then, the characteristics of the device were evaluated.

2.7. Fabrication of flexible PSCs by spin coating method

For comparison with the device, which was fabricated by the patternable brush painting method, another device was fabricated by the spin-coating method. After cleaning the patterned ITO PET substrate, UVO cleaning was performed for about 10 min to decrease the work function of ITO. An approximately 40 nm-thick film was obtained after spin-coating PEDOT: PSS on the ITO PET substrate at 4000 rpm. Then, it was annealed on a hot plate at 120 °C for about 20 min to remove the residual solvent. The donor material, P3HT, and acceptor material, $PC_{61}BM$, were blended in ortho-dichlorobenzene (ODCB) at a ratio of 1:0.6 and a concentration of 3.0 wt% and heated at 90 °C for about 30 min. An approximately 130 nm-thick film was obtained on PEDOT: PSS after spin coating at 500 rpm. Then, it was annealed on a hot plate at 160 °C for about 10 min. As in the case of the patternable brush painting method, BaF_2 (0.1 Å/s, 2 nm), Ba (0.2 Å/s, 2 nm) and Al (5 Å/s, 100 nm) were thermally deposited in a high vacuum chamber and encapsulated in that order.

2.8. Characterization of flexible PSCs

The device evaluation was performed at 298 K using a Class A Oriel solar simulator (Oriel 96000 150 W solar simulator) having a xenon lamp that simulates AM 1.5G irradiation (100 mW/cm^2) from 400 to 1100 nm. The instrument was calibrated with a monocrystalline Si diode fitted with a KG3 filter to bring the spectral mismatch to unity. The calibration standard was calibrated by the National Renewable Energy Laboratory (NREL).

3. Results and discussion

Fig. 1 shows the structure of the polymer photovoltaic cell and the chemical structures of P3HT and PCBM used in this paper. The materials, device fabrication process and device characterization are described in the experimental part in detail. Scheme 1 describes the patternable brush painting process used in this study. As the substrate, an ITO-PET substrate instead of an ITO glass substrate was used to make a flexible electronic device. In addition, a repositionable adhesive (3M) was used to pattern the PEDOT: PSS and photo active layers. After covering the patterned ITO PET substrate with the repositionable adhesive-coated metal mask, brush painting was performed. The two layers were completely glued in order to preclude the possibility of the capillary phenomenon occurring between the PET substrate and metal mask due to the repositionable adhesive. As shown in Fig. 2b, perfect brush painting was observed in the active layer-patterned parts only. Because the metal mask is weaker than PET in terms of its surface energy, the adhesion of the repositionable adhesive to the metal mask was much stronger than that to the PET substrate. Consequently, it was possible to cleanly remove the metal mask from the PET substrate. Furthermore, the repositionable adhesive-coated metal mask could be repeatedly used, and the repositionable adhesive residues were easily removed using hexane.

As shown in Fig. 1a, for the device structure of the flexible PSCs, a 40 nm-thick PEDOT: PSS layer was formed on the patterned ITO PET using a brush painting method and annealed at 120 °C, as shown in Scheme 1. Then, the residual solvent was removed. Under the same method, a photo-active layer was formed using the photo-active ink. Fig. 3 shows the change in the thickness of the PEDOT: PSS and photo-active layers caused by the change in the brush painting speed rate. The thickness

decreased in a linear manner as the brush painting speed rate (cm/s) increased, regardless of the concentration and type of solute and solvent. In other words, the brush painting speed rate is a crucial factor in determining the thickness of the layer in the brush painting method. When the speed was increased three times, the thickness decreased 1.5–2 times. Consequently, it was possible to obtain patterning process-enabled PSCs using the brush painting method. In addition, for comparison with the patternable brush painting flexible PSCs, another device was fabricated by the conventional spin coating method. A device with a 40 nm PEDOT: PSS and 130 nm active layer, which had the structure shown in Fig. 1a was fabricated by the spin coating method. The characteristics of the devices, which were fabricated by the brush painting and spin coating methods were compared as a function of the annealing temperature of the photo-active layer (100–160 °C). To form the cathode on the photo-active layer, lastly, BaF_2 (0.1 Å/s, 2 nm), Ba (0.2 Å/s, 2 nm) and Al (5 Å/s, 200 nm) were thermally deposited in a high vacuum chamber (1×10^{-6} Torr or less). BaF_2 was applied as an electron transporting layer to effectively collect the electrons through an Ohmic contact between photo-active layer and cathode. In addition, Ba (−2.7 eV), a low work function material was used as the cathode. A 100 nm thick layer of Al was deposited to protect the cathode. The current density–voltage (*J–V*) characteristics and incident photon to current conversion efficiency (IPCE) are shown in Fig. 4(a, b), and the results are listed in Table 1.

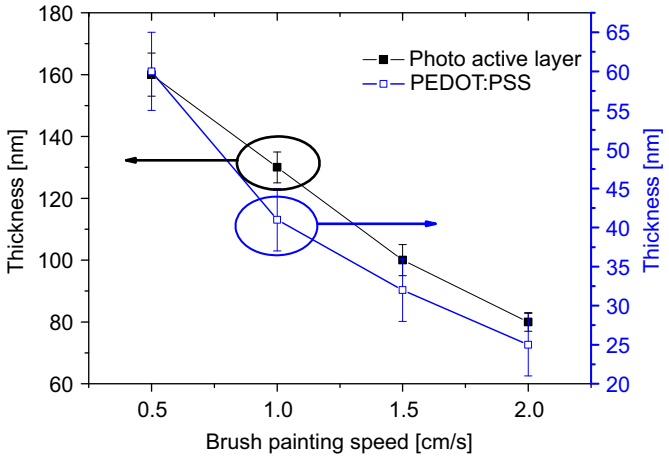

Fig. 3. Thickness of active layer and PEDOT: PSS layer by brush painting speed.

In the case of the device which was fabricated by the spin-coating method, the highest efficiency was observed when the annealing temperature was 160 °C. Its Jsc, Voc and FF values were 7.3 mA/cm^2, 0.616 V and 40.7%, respectively. Even though there was no change in Voc despite the change in temperature, FF was increased compared to the case where the temperature was 120 °C. In particular, the Jsc and PCE values of photo-active layer more than doubled as the thermal treatment temperature increased from 120 to 160 °C because of the improvement of the crystallinity in P3HT. When the annealing temperature was 120 °C, the series resistance (Rs) was 102 Ω cm^2. However, it decreased to 41 Ω cm^2 at 160 °C. A decrease in Rs means a decrease of the internal resistance. The Jsc was improved due to the increase in the characteristics of charge transport after the improvement of the crystallinity in P3HT. In addition, the increase in the shunt resistance (Rsh) led to an improvement in FF. Because the thermal treatment temperature for P3HT has more effect on the crystallinity in the spin coating method, however, the impact of the improvement in FF on improvement of the PCE was minor.

In the case of the device fabricated using the brush painting method, on the other hand, the highest power conversion efficiency (PCE) of 2.6% was observed for the device which was annealed at 120 °C after brush painting. Here, the Jsc, Voc and FF values were 8.5 mA/cm^2, 0.636 V and 48.8%, respectively. When the annealing temperature was increased from 100 to 120 °C, the Voc as well as the Jsc and FF significantly increased, which in turn

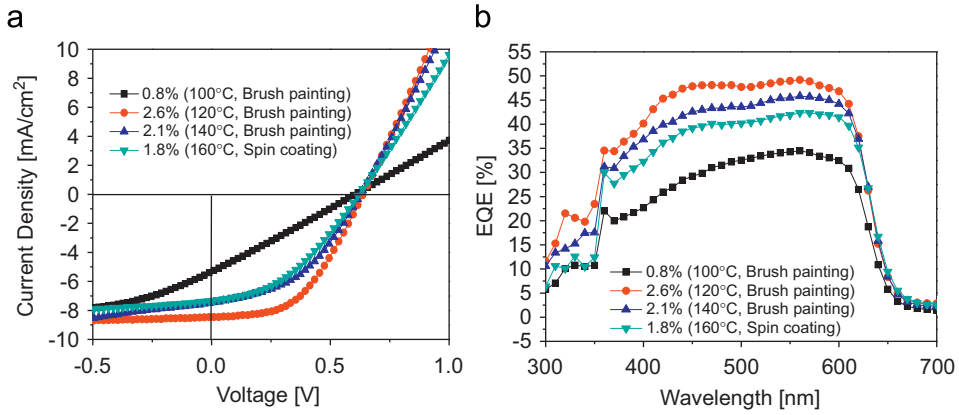

Fig. 4. (a) *J–V* characteristics of flexible PSCs with different fabrication methods and annealing temperatures under 100 mW/cm^2 illumination. (b) IPCE spectra of flexible PSCs with different fabrication methods and annealing temperatures.

Table 1
Characteristics of devices.

Annealing Temp. [°C]		Jsc [mA/cm^2]	Voc [V]	FF [%]	PCE [%]	Series resistance R_s Ω [cm^2]	Shunt resistance R_{sh} Ω [cm^2]
Brush painting method	100	5.2	0.595	26.6	0.8	106	134
	120	8.5	0.636	48.8	2.6	29	2019
	140	7.4	0.636	43.5	2.1	33	403
Spin coating method	120	3.5	0.616	37.4	0.8	102	150
	140	6.9	0.616	38.4	1.6	62	465
	160	7.3	0.616	40.7	1.8	41	673

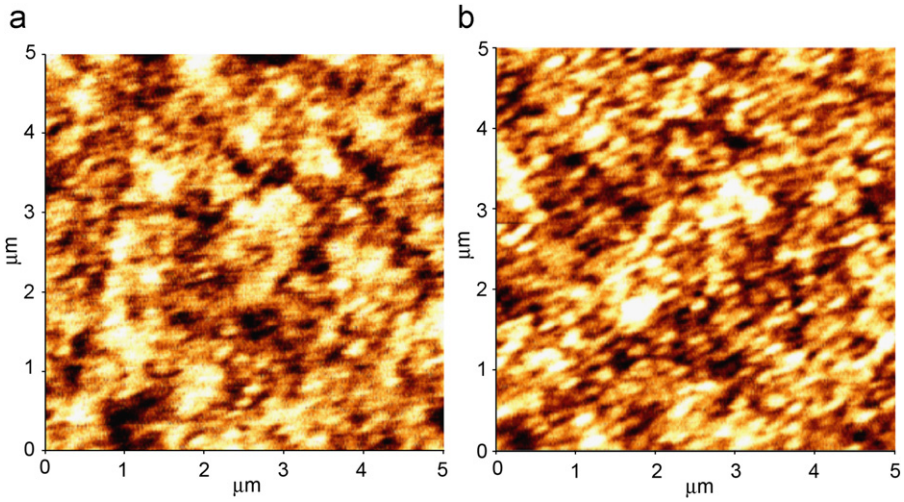

Fig. 5. AFM image of active layers. (a) active layer coated by brush painting (RMS: 0.19 nm) (b) Active layer coated by spin coating (RMS: 0.19 nm).

brought about an increase in the PCE. In particular, the increase in the Voc was larger in the device, which was fabricated by the spin-coating method. The device fabricated using the brush painting method was better than that by the spin coating method in terms of the alignment of P3HT in the active layer and improvement of the interchain interaction. As a result, an improvement of the Voc was observed.

In addition, Jsc and FF were dramatically increased as well, while Rs was the lowest with a value of 29 $\Omega\,cm^2$. In other words, an Ohmic contact occurred at the interface in each layer. In terms of Rsh, the highest value of 2018 $\Omega\,cm^2$ was observed. Furthermore, the decrease in the charge recombination was confirmed at the BHJ/metal interface. Thanks to the decrease in Rs and increase in Rsh, both the Jsc and FF values increased. As a result, the PCE improved. However, the Voc stayed the same even when the annealing temperature was increased to 140 °C. However, both the Jsc and FF decreased due to the increase in Rs and decrease in Rsh, which in turn caused a decrease in the PCE.

Fig. 5 shows the AFM images of the devices, which were fabricated by brush painting (5a) and spin coating (5b) after annealing. In both methods, a root mean square (RMS) of 0.19 nm was observed. However, it was confirmed that the brushing process enhanced the ordering of the polymers. In the brushing process, the shear stress among the polymer chains had the biggest impact on the ordering of the polymers. In Newtonian polymer solutions, the shear stress (τ) is in proportion to the velocity gradient (Δv) and viscosity (υ) ($\tau = \Delta v \times \upsilon$). In the case of spin coating, the Δv of the polymer solution and air boundary is '0' ($\tau = 0$) [24]. In the case of brush painting, on the other hand, even shear stress was observed in all of the polymer solution sections, due to the effective contact between the brush and polymer solution (Δv = constant) [25]. Therefore, when the brushing process was used, it was easier to form a channel through which the holes and electrons in the photo-active layer can move. Compared to the spin coating method Rs decreased from 41 to 29 $\Omega\,cm^2$, while Jsc increased from 7.3 to 8.5 mA/cm^2. The Rsh and FF values also increased from 673 to 2019 $\Omega\,cm^2$ and from 40.7% to 48.8% respectively. In consequence, the PCE increased by 44% (from 1.8% to 2.6%).

4. Conclusion

In this study, flexible PSCs were successfully fabricated by a patterning process of hole-transporting and photo-active layers using a repositionable adhesive. Because the metal mask has a lower surface energy than PET, the repositionable adhesive adheres much more strongly to the metal mask. Consequently, it was possible to cleanly remove the metal mask from the PET substrate. By means of this simple method, the efficiency of the patternable brush painting device with a PCE of 2.6% was improved by 44%, compared to the conventional device in which the spin coating method was used.

Acknowledgement

This research was supported by a grant(10037195) from the Fundamental R&D Program for Core Technology of Materials funded by the Ministry of Knowledge Economy, Republic of Korea.

References

[1] D. Placencia, W. Wang, R.C. Shallcross, K.W. Nebesny, M. Brumbach, N.R. Armstrong, Organic photovoltaic cells based on solvent-annealed, textured titanyl phthalocyanine/C_{60} heterojunctions, Adv. Funct. Mater. 19 (2009) 1913–1921.
[2] S.O. Jeon, J.Y. Lee, Improved high temperature stability of organic solar cells using a phosphine oxide type cathode modification layer, Sol. Energy Mater. Sol. Cells 95 (2011) 1102–1106.
[3] C. Shi, Y. Yao, Y. Yang, Q. Pei, Regioregular copolymers of 3-alkoxythiophene and their photovoltaic application, J. Am. Chem. Soc. 128 (2006) 8980–8986.
[4] J.Y. Lee, W.S. Shin, J.R. Haw, D.K. Moon, Low band-gap polymers based on quinoxaline derivatives and fused thiophene as donor materials for high efficiency bulk-heterojunction photovoltaic cells, J. Mater. Chem. 19 (2009) 4938–4945.
[5] J.Y. Lee, S.W. Heo, H. Choi, Y.J. Kwon, J.R. Haw, D.K. Moon, Synthesis and characterization of 2,1,3-benzothiadiazole-thieno [3,2-b] thiophene-based charge transferred-type polymers for photovoltaic application, Sol. Energy Mater. Sol. Cells 93 (2009) 1932–1938.
[6] J.Y. Lee, M.H. Choi, S.W. Heo, D.K. Moon, Synthesis of random copolymers based on 3-hexylthiophene and quinoxaline derivative: influence between the intramolecular charge transfer (ICT) effect and π-conjugation length for their photovoltaic properties, Synth. Met. 161 (2011) 1–6.
[7] J.Y. Lee, M.H. Choi, H.J. Song, D.K. Moon, Random copolymers based on 3-hexylthiophene and benzothiadiazole with induced π-conjugation length and enhanced open-circuit voltage property for organic photovoltaics, J. Polym. Sci. Part A: Polym. Chem. 48 (2010) 4875–4883.
[8] L. Dai, H.J. Griesser, A.W.H. Mau, Surface modification by plasma etching and plasma patterning, J. Phys. Chem. B 101 (1997) 9548–9554.
[9] S. Steudel, K. Myny, S.D. Vusser, J. Genoe, P. Heremans, Patterning of organic thin film transistors by oxygen plasma etch, Appl. Phys. Lett. 89 (2006) 183503-1–183503-3.
[10] N.E. Sosa, J. Liu, C. Chen, T.J. Marks, M.C. Hersam, Nanoscale writing of transparent conducting oxide features with a focused ion beam, Adv. Mater. 21 (2009) 721–725.

[11] F.C. Krebs, Fabrication and processing of polymer solar cells: a review of printing and coating techniques, Sol. Energy Mater. Sol. Cells 93 (2009) 394–412.
[12] J. Alstrup, M. Jørgensen, A.J. Medford, F.C. Krebs, Ultra fast and parsimonious materials screening for polymer solar cells using differentially pumped slot-die coating, ACS Appl. Mater. Interfaces 2 (2010) 2819–2827.
[13] E. Bundgaard, O. Hagemann, M. Manceau, M. Jørgensen, F.C. Krebs, Low band gap polymers for roll-to-roll coated polymer solar cells, Macromolecules 43 (2010) 8115–8120.
[14] M. Manceau, D. Angmo, M. Jørgensen, F.C. Krebs, ITO-free flexible polymer solar cells: from small model devices to roll-to-roll processed large modules, Org. Electron 12 (2011) 566–574.
[15] F.C. Krebs, J. Fyenbob, M. Jørgensen, Product integration of compact roll-to-roll processed polymer solar cell modules: methods and manufacture using flexographic printing, slot-die coating and rotary screen printing, J. Mater. Chem. 20 (2010) 8994–9001.
[16] F.C. Krebs, Roll-to-roll processing and product integration of polymer solar cells, Energy Environ. Sci. 3 (2010) 512–525.
[17] G. Li, V. Shrotriya, Y. Yao, Y. Yang, Investigation of annealing effects and film thickness dependence of polymer solar cells based on poly(3-hexylthiophene), Appl. Phys. Lett 98 (2005) 043704-1–043704-5.
[18] X. Yang, J. Loos, S.C. Veenstra, W.J.H. Verhees, M.M. Wienk, J.M. Kroon, M.A.J. Michels, R.A.J. Janssen, Nanoscale morphology of high-performance polymer solar cells, Nano Lett. 5 (2005) 579–583.
[19] T. Aernouts, T. Aleksandrov, C. Girotto, J. Genoe, J. Poortmans, Polymer based organic solar cells using ink-jet printed active layers, Appl. Phys. Lett. 92 (2008) 033306-1–033306-3.
[20] J.H. Huang, Z.Y. Ho, T.H. Kuo, D. Kekuda, C.W. Chu, K.C. Ho, Fabrication of multilayer organic solar cells through a stamping technique, J. Mater. Chem. 19 (2009) 4077–4080.
[21] D.H. Wang, D.G. Choi, K.J. Lee, O.O. Park, J.H. Park, Active layer transfer by stamping technique for polymer solar cells: Synergistic effect of TiO_x interlayer, Org. Electron. 11 (2010) 599–603.
[22] S.S. Kim, S.I. Na, J. Jo, G. Tae, D.Y. Kim, Efficient polymer solar cells fabricated by simple brush painting, Adv. Mater. 19 (2007) 4410–4415.
[23] S.S. Kim, S.I. Na, S.J. Kang, D.Y. Kim, Annealing-free fabrication of P3HT: PCBM solar cells via simple brush painting, Sol. Energy Mater. Sol. Cells 94 (2010) 171–175.
[24] R.B. Bird, W.E. Stewart, E.N. Lightfoot, Transport Phenomena, John Wiley & Sons, New York, NJ, 1960 Chapter. 2.
[25] C.C. Mell, S.R. Finn, Forces exerted during the brushing of a paint, Rheol. Acta. 4 (1965) 260–261.